Computer-aided limit states analysis of bridge abutments

Murat Dicleli

Assistant Professor
Department of Civil Engineering and Construction
Bradley University, Peoria, Illinois 61625, USA
Email: mdicleli@usa.net

ABSTRACTS

This paper presents a computer program developed for limit states analysis of abutments. The program can perform both structural and geotechnical analysis of bridge abutments and check their resistances in compliance with limit states design criteria. In the program, the earth pressure coefficient for the backfill soil is calculated as a function of abutment's lateral non-linear displacement. Therefore, for abutments partially restrained against lateral movement, an earth pressure coefficient less than that of at-rest conditions may be obtained. This may result in a more economical design.

KEYWORDS

Bridge, abutment, foundation, limit-state-design, soil-structure-interaction, optimization

1. Introduction

Limit states are conditions under which a structure can no longer perform its intended functions. The limit states design (LSD) process considers two conditions to satisfy; the ultimate and the serviceability limit states. The ultimate limit states (ULS) are related to the safety of the structure and they define the limits for its total or partial collapse. The serviceability limit states (SLS) represent those conditions, which adversely affect the expected performance of the structure under service loads.

LSD has received particular attention in the geotechnical and structural engineering literature over the last three decades. Many researchers and practicing engineers have documented their findings on this subject [1-18]. Guidance with the application of limit state design procedures is available through a number of design codes [19-22]. However, the application of LSD to substructures is more recent. In the past, substructure design was based on allowable stress or working stress design (WSD), while the superstructure design was based on LSD. The use of LSD philosophy for superstructures and WSD philosophy for substructures led to confusions. The confusion potentially exists with respect to loading at soil-structure interface for the evaluation of ultimate limit states (ULS). The structural engineer employing the LSD approach for the design of substructures thinks in terms of factored loads to be supported by the bearing soil. The geotechnical engineer using WSD approach in soil bearing capacity assessment thinks in terms of nominal loads and allowable soil pressures. Therefore, the geotechnical report provides the structural engineer with the values of allowable soil pressure. The structural engineer then interprets the meaning of the recommended soil pressure and factors it in an effort to compare it with the responses due to factored structural loads. Nevertheless, the recommended soil bearing pressure may be controlled by settlement considerations or SLS rather than bearing failure considerations or ULS. Obviously, a sense for the actual level of safety has been lost through the incompatible design process. The foundation may be over-

designed resulting in loss of economy rather than the improved economy that LSD is supposed to provide. Therefore, it became evident that a limit state approach was required for geotechnical design.

The LSD process for the design of bridge abutments is more tedious than WSD process. It requires two different analyses to satisfy the structure performance for both SLS and ULS. The ULS itself requires more than one analysis to satisfy the geotechnical and the structural limit states. Generally, designers try to obtain the optimal structure dimensions to satisfy the limit states criteria by following a trial-and-error analysis and design procedure. Nevertheless, a manually performed trial-and-error analysis and design iteration to obtain the optimal structure dimensions and reinforcement under different loading conditions and given limit states criteria could be inaccurate, tedious and time consuming. Considering these, a computer program, ABA, for the analysis and design of bridge abutments has been developed.

In the subsequent sections, first, the general features of the program, ABA are described. This is followed by a brief description of the general program structure. Next, the procedure used in the program for calculating backfill pressure coefficient is defined. Then, the LSD procedure implemented in the program for bridge abutment design is introduced. This included the procedure for checking the stability of the structure for sliding and overturning and the calculation of base pressure, pile axial forces, structural responses and resistances. Following this, simple design-aid charts for retaining walls are introduced.

2. General features of the program

ABA is capable of analyzing bridge abutments and retaining walls and checking their structural and geotechnical resistance using LSD criteria. Retaining walls are programmed as a sub-element of abutments and therefore the word abutment will mean both retaining wall and abutment thereafter.

2.1 Abutment Geometry

ABA analyses the general type of reinforced concrete abutment shown in Figures 1(a) and (b). The generic shape of the abutment's wing-wall is defined in Fig. 1(c). In the program, the geometry of the abutment can be modified by assigning constraints to its dimensions. The ballast-wall and the breast-wall parts of the abutment obtained by assigning various constraints to their dimensions are illustrated in Figures 2(a) and (b).

The geometry and local coordinate axes of the abutment footing are shown in Fig.3. For abutments with deep foundations, piles are defined in rows extending along X2 footing local coordinate axes as shown in Figures 4(a) and (b). The number of piles in a row and the location of each row from the centroid of the footing are input by the user. Each row may have piles with identical batters perpendicular to row direction. If a row contains piles with different batters, then it may be defined as a combination of two or more rows of piles located at the same distance from the centroid of the footing. The piles at both ends of each row may also have batters parallel to row direction. The piles are assumed to have constant spacing within a row and located symmetrically with respect to the X1 footing local coordinate axis.

2.2 Loads

The types of loads allowed by the program to act on the abutments are; concentrated loads at the bearings, surcharge pressure, backfill soil pressure, soil compaction load, self weight of the abutment, backfill soil and barrier walls on wing-walls. The concentrated loads may belong to one of permanent, transitory or exceptional load groups shown in Table 1. Surcharge pressure is assumed to act over the entire surface area of the backfill soil at the abutment top level. It may

belong to either permanent or transitory load group. The backfill soil pressure is either calculated internally by the program as a function of structure lateral displacement or it can be defined externally by the user. The user defines compaction load at the surface of the backfill soil. The program then internally defines the linearly varying lateral earth pressure due to this compaction load. The program also internally calculates the self-weight of the abutment, backfill soil, and barrier-walls-on-wing-walls.

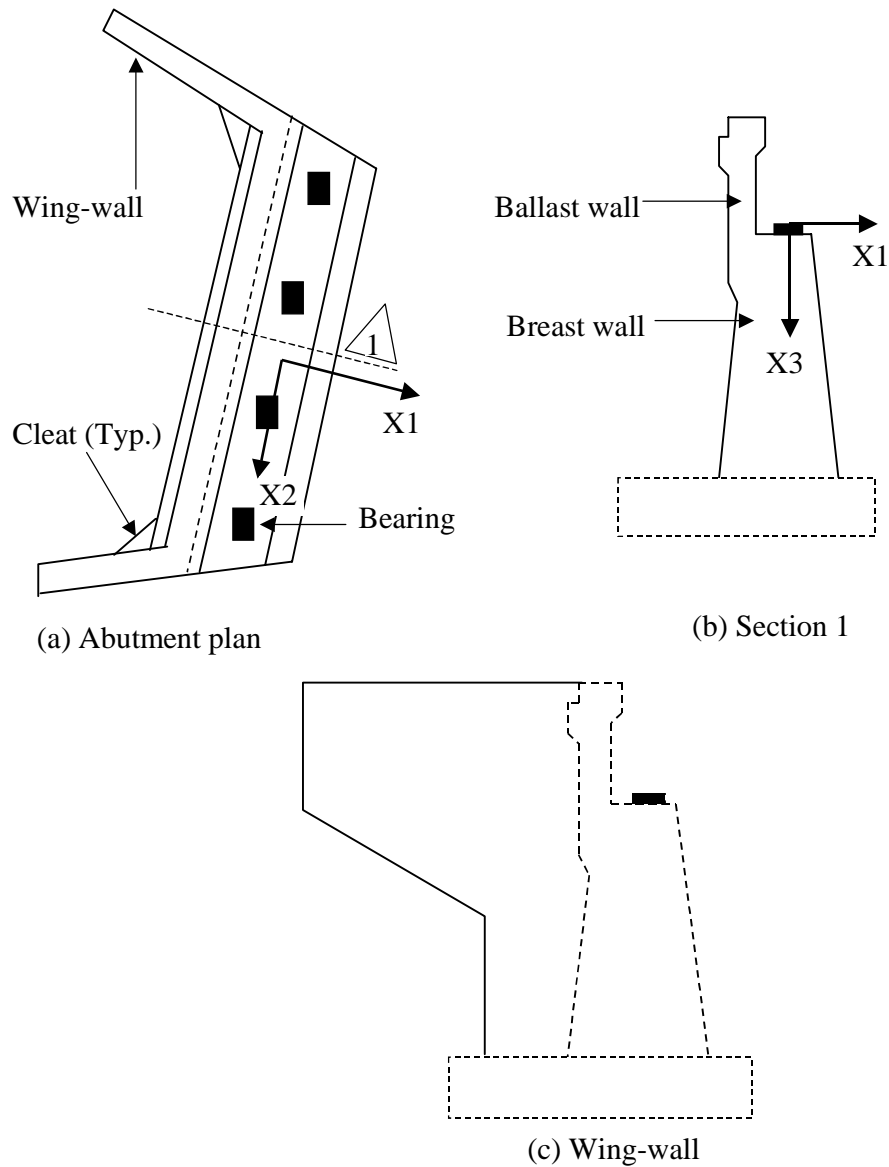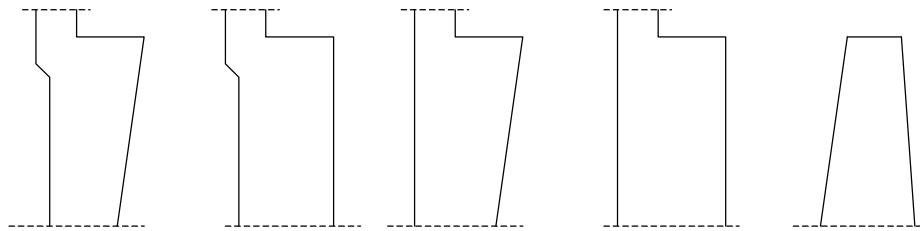(a) Abutment plan

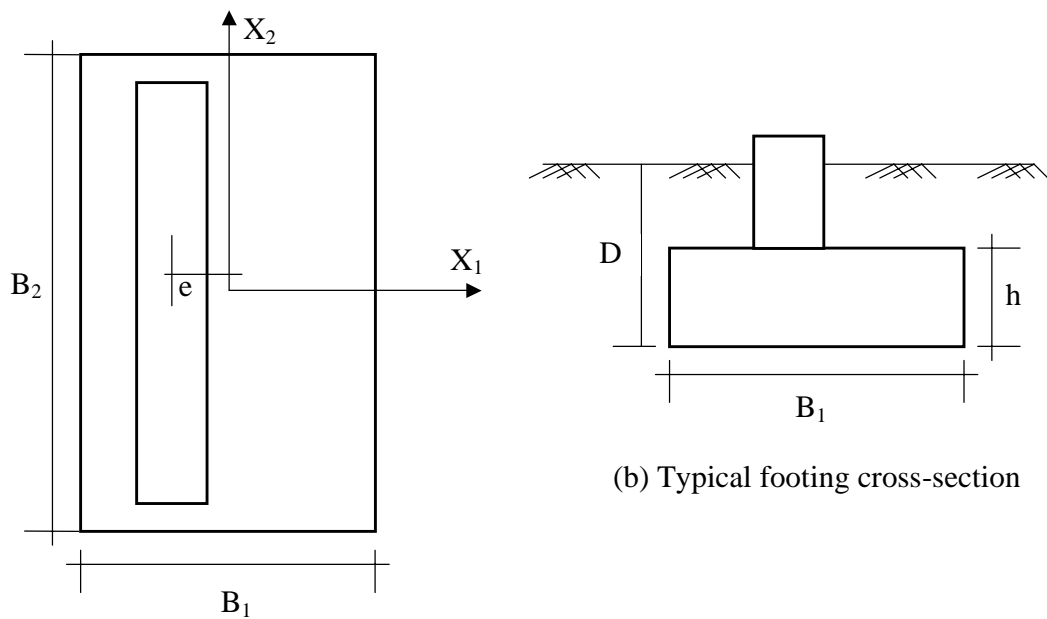(b) Section 1

(c) Wing-wall

Fig. 1 - Abutment geometry

(a) Ballast wall geometric configuration

(b) Breast wall geometric configuration

Fig. 2 - Geometric configurations of ballast and breast walls

(b) Typical footing cross-section

(a) Abutment footing plan

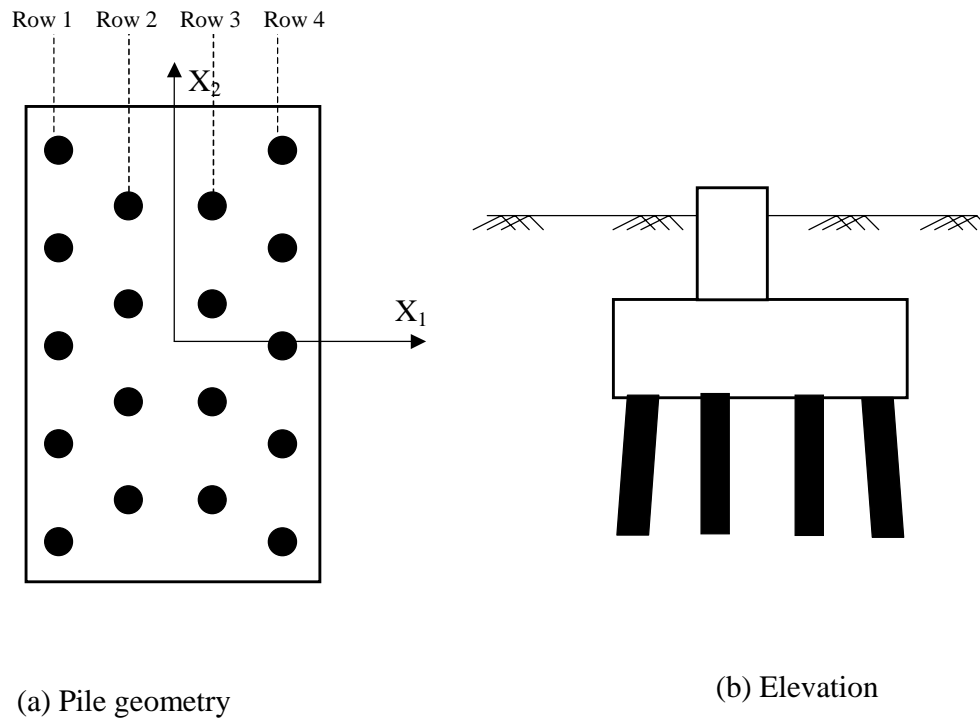**Fig. 3** - Footing geometry

(a) Pile geometry

(b) Elevation

Fig. 4 - Pile geometry for deep foundations

3. General program structure

ABA consists of a control program that manages the database, an analysis and design engine and a graphical user interface (GUI) for user data input. Fig. 5 illustrates the program structure. The analysis and design engine consists of three modules; abutment analysis module, footing analysis module and resistance module. The abutment analysis module performs the analysis of the abutments excluding the footing part. The footing analysis module then performs the analysis for the footing part of the abutment or it can be operated independently. The resistance module then calculates the structural resistance of any specified cross-section on the structure. As shown in Fig. 5, the control program first allows the user to define the properties of the abutment and its footing using the GUI. The user-defined data is then stored in a structured database, which contains material, geometry, loading data and control flags. The program then uses this database for the analysis and design of the abutment. The control program operates the necessary sub-module depending on the analysis type. If footing is analyzed as part of abutment, then the control program first initiates the abutment analysis module. Next, it stores the footing load data, obtained from the abutment analysis module, in the database. Then, it calls the footing analysis module to complete the analysis. Finally, it calls the resistance module to perform structural resistance calculations.

4. Calculation of earth pressures

In the program, separate earth pressure conditions are considered behind the abutment for geotechnical and structural LSD. For the geotechnical LSD, active earth pressure condition is considered behind the abutment as the structure is assumed to rotate at its base or displace away from the backfill at the verge of geotechnical limit state conditions such as overturning or sliding of the structure. Such movements will mobilize the soil to an active state of equilibrium. For structural LSD, the structure is assumed to have no such movements. Accordingly, an earth

pressure ranging between active and at-rest conditions is considered for the structural design of the abutment.
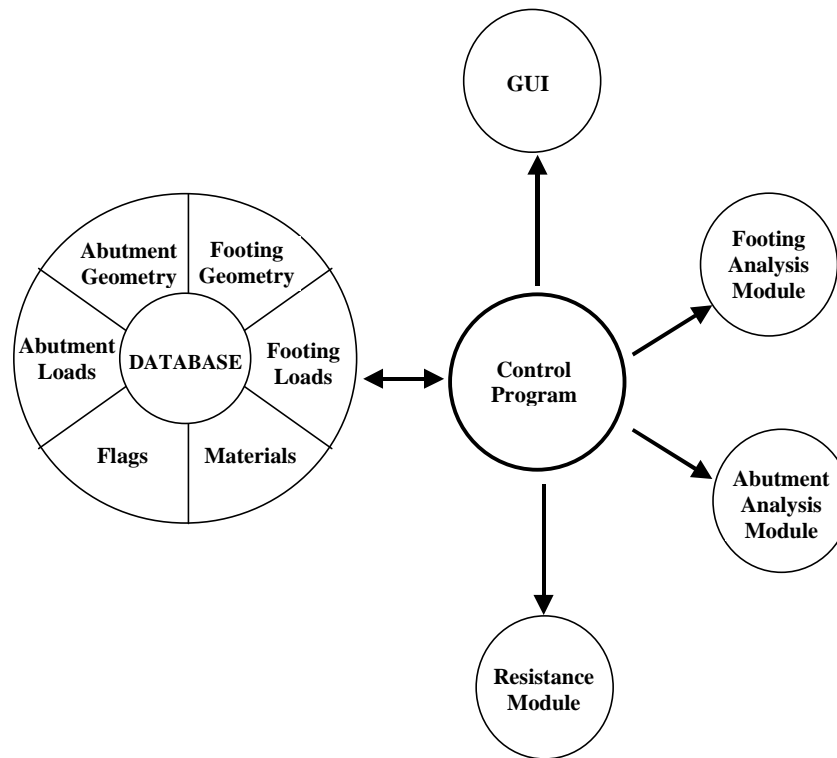

Fig. 5 - Program structure

The actual earth pressure coefficient, K, may change between active, K_a and at-rest, K_o, earth pressure coefficients depending on the amount of lateral deformation of the abutment due to the permanently applied loads. Past researchers obtained the variation of earth pressure coefficient as a function of structure top displacement from experimental data and finite element analyses [17, 23]. For practical purposes, this variation is assumed as linear as shown in Fig. 6. This linear relationship is expressed as:

$$K = K_o - \varphi d \geq K_a \tag{1}$$

Where, d is the top displacement of the earth retaining structure away from the backfill soil and v, is the slope of the earth pressure variation depicted in Fig. 6. The calculated top displacement of the abutment and the active and at-rest earth pressure coefficients are substituted into the above equation to obtain the actual earth pressure coefficient for the structural design. A similar approach was followed elsewhere [24, 25] to estimate the passive earth pressure coefficient for the backfill soil for the design of integral-abutment bridges. In the program, Coulomb theory [26] is used to calculate the active and at-rest lateral earth pressure coefficients assuming zero friction between the wall surface and the backfill. The effect of backfill slope on the active earth pressure coefficient is also considered in the program.

Structure Model

The structure models shown in Fig. 7 are used in the program for the calculation of abutment top displacement. Only the effects of unfactored dead loads and backfill pressure are considered in the calculations. The eccentricities due to the dead load reactions on the bearings are also taken into consideration by applying a concentrated moment at the point of application of the dead loads on the structure model. The abutment is modeled as a cantilever having a unit width and a variable cross-section along its height. The cantilever element is then connected to the footing member. The footing is modeled as a vertical rigid bar with a rotational spring

connected to its end. The length of this rigid bar is set equal to the footing depth, h_f. The rotational spring at the end of the rigid bar simulates the effect of footing rotation on the magnitude of abutment top displacement. The loads acting on the abutment are proportioned to the unit width of the abutment.
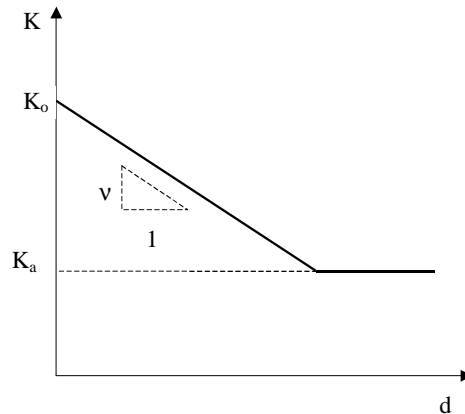
Fig. 6 - Variation of earth pressure coefficient as a function of abutment displacement

| (a) Abutment | (b) Abutment model with elastomeric bearings | (c) Abutment model with frictional bearings |
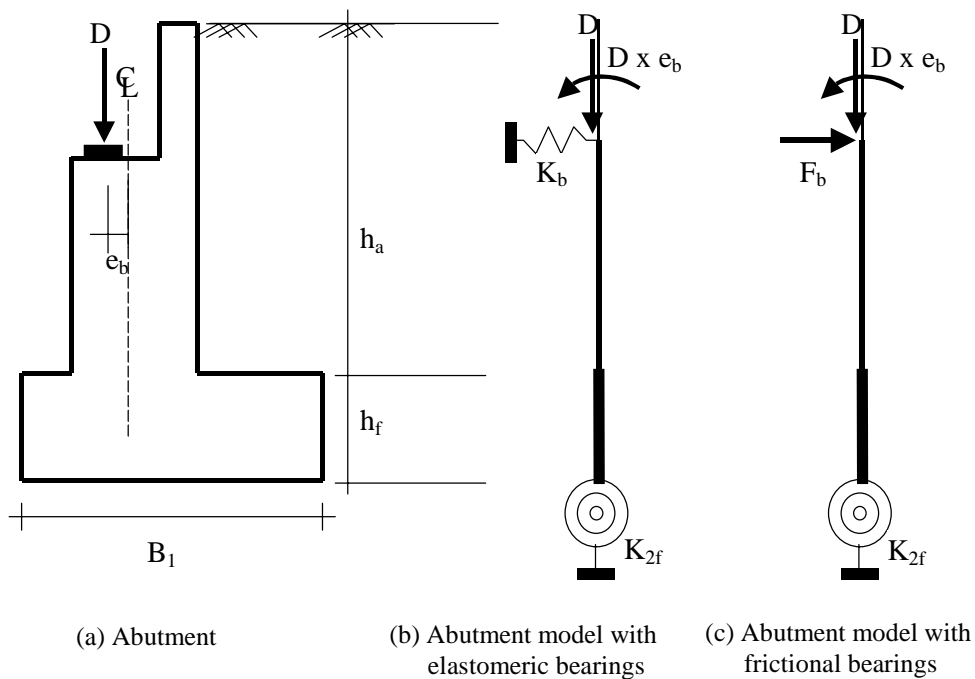
Fig. 7 - Structure model for the calculation of abutment displacement

The bridge deck may restrain the lateral displacement of the abutment. The degree of this restraint is based on the type of bearings used. For frictional bearings, the restraining force is equal to the total dead load reaction force on the bearing, multiplied by the coefficient of friction for the type of bearing used. In the program, first a fictitious rigid lateral support is introduced in the structure model at the bearing location. Next, the lateral reaction force due to the applied loads is calculated at this support. If the restraining force provided by the bearings is smaller than this reaction force, it is applied at the bearings' location in the model as shown in Fig. 7. Otherwise, the movement is assumed to be totally restrained and the earth pressure coefficient is set equal to K_o. For elastomeric bearings, the restraining force is proportional to

the lateral displacement of the abutment at bearing's location and the stiffness of the bearing. A spring with stiffness identical to that of the elastomeric bearings is placed at the bearing location as shown in Fig. 7 to simulate the restraining effect of the bearings. The stiffness of this spring per unit width of abutment is expressed in the program as:

$$K_b = \frac{n_b G_b A_b}{h_b w_a} \tag{2}$$

Where, n_b is the number of bearings, G_b is the shear modulus of the bearing material, A_b is the plan area of the bearing, h_b is the bearing height and w_a is the total width of the abutment.

For bearings providing lateral fixity at the abutments, the movement is assumed to be restrained and the earth pressure coefficient is set equal to K_o. In the case of cantilever retaining walls, no restraint is considered in the displacement calculation.

The stiffness of the rotational spring in the model is determined by the rotational stiffness of the footing. For shallow foundations, the rotational stiffness, $K_{\theta f}$, of the footing is expressed as [27]:

$$K_{\theta f} = \frac{1}{12} B_1^3 B_2 k_s \tag{3}$$

Where, B_1 and B_2 are the plan dimensions of the footing respectively parallel and perpendicular to the bridge longitudinal directions and k_s is the coefficient of sub-grade reaction for the bearing soil input by the user. In the case of pile foundations, the rotational stiffness of the foundation is calculated in the program as [27]:

$$K_{\theta f} = \sum_{i=1}^{nr} n_i \frac{E_p A_p}{L_p} d_i^2 \tag{4}$$

Where, nr is the number of pile rows, E_p is the modulus of elasticity of pile material, A_p and L_p are respectively, the cross-sectional area and length of a single pile and d_i is the distance of pile row i, from the geometric centerline of the footing.

A closed form solution for the reaction forces at the translational and rotational springs in the model is obtained for each type of load applied on the structure and implemented in the program.

Calculation of Top Displacement

The displacement, δ^*_T, at the top of the abutment is calculated in the program using the following equation.

$$\delta_T = \frac{M_b}{K_{\theta f}} (h_a + h_f) + \int_0^{h_a} m \frac{M}{E_c I_a} dx \tag{5}$$

Where, M_b is the total moment at the footing base, M and m are moments, respectively, due to the externally applied loads and a horizontal unit dummy load applied at the top of the abutment, E_c is the modulus of elasticity of abutment concrete and I_a and h_a are respectively the moment of inertia and height of the abutment. The first set of terms in the above equation represents the contribution of footing rotation to the top displacement. The integration represents the contribution of the abutment's flexural deformation to the top displacement and is obtained using the unit dummy load method [28]. Note that the expression, M/E_cI_a, in the integral is the curvature of the abutment due to the applied loads. The integration is performed numerically using the trapezoidal rule of numerical integration method [29]. The structure model is first divided into 100 segments and the resulting segment length is used as an integration step. The moment, M, due to externally applied loads is then calculated at each point of integration. Next, the inelastic curvature ($\phi = M/E_cI_a$) corresponding to the applied

moment and axial force is calculated using nonlinear material models for concrete and steel to obtain an accurate estimate of structure displacement. The procedure followed to calculate the curvature is defined in the subsequent sections. The moment, *m*, due to the unit dummy load is also calculated at the integration points and multiplied by the calculated curvature and an integration factor which is a function of the type of numerical integration method used. For this particular case, the integration factor is 0.5 for the first and last points of integration and 1.0 for the rest. Finally, the top displacement due to the flexural deformation of the abutment is obtained by summing up the results obtained for each integration point and multiplying the sum by the integration step.

Material Models

In the calculation of non-linear curvatures, the following constitutive relationship is used for concrete stress, f_c, in compression, as a function of concrete strain ε_c [30]:

$$f_c = f_{co}^{'} \left[\frac{2\varepsilon_c}{\varepsilon_{o1}} - \left(\frac{\varepsilon_{085}}{\varepsilon_{01}} \right)^2 \right] \qquad for \quad \varepsilon_c \le \varepsilon_{01} \qquad (6)$$

$$f_c = f_{co}^{'} - (\varepsilon_c - \varepsilon_{o1}) \left(\frac{0.15 f_{co}^{'}}{\varepsilon_{085} - \varepsilon_{01}} \right) \qquad for \quad \varepsilon_{01} < \varepsilon_c \le \varepsilon_{cu} \qquad (7)$$

Where, $f^{''}_{co}$ is the specified strength of abutment concrete, ε_{01}, and ε_{085} are the strains at peak and 85% of the peak strength.

For concrete stress in tension, the following linear constitutive relationship is used:

$$f_c = \varepsilon_c E_c \qquad\qquad for \quad \varepsilon_c \le \varepsilon_{cr} \qquad (8)$$

$$f_c = 0 \qquad\qquad for \quad \varepsilon_c > \varepsilon_{cr} \qquad (9)$$

Where, E_c is the modulus of elasticity of concrete and is expressed as:

$$E_c = 5000 \sqrt{f_{co}^{'}} \qquad (10)$$

ε_{cr} is the strain at cracking and is expressed by the following equation;

$$\varepsilon_{cr} = \frac{\sqrt{f_{co}^{'}}}{2E_c} \qquad (11)$$

For the stress, f_s, in reinforcing steel, the following elasto-plastic stress-strain relationship is assumed.

$$f_s = \varepsilon_s E_s \qquad\qquad for \quad \varepsilon_s \le \varepsilon_y \qquad (12)$$

$$f_s = f_y \qquad\qquad for \quad \varepsilon_s > \varepsilon_y \qquad (13)$$

The strain hardening part of the stress-strain relationship for steel is not considered in the above equations, since under service loads the stress in steel will not reach the strain hardening region.

Calculation of Moment Curvature Relationship

In the program, to calculate the curvature corresponding to an applied moment, M, and an axial force, P, at a cross-section along the abutment, first, an extreme fiber compressive strain, ε_{cu}, is assumed for concrete as shown in Fig. 8. The slope of the strain diagram is established for an assumed location, c, of neutral axis measured from the top of the section. Corresponding compressive and tensile stresses in concrete and steel are determined from material models described above. Internal forces in concrete, as well as reinforcing steel are calculated. The section is divided into rectangular strips for the purpose of calculating compressive forces in concrete as shown in Fig. 8. First, the concrete stress at the middle of each strip is calculated and multiplied by the area of the strip. Then, the results are summed up to obtain the total force

due to compressive concrete stresses. To calculate the tensile forces in concrete, first, the depth of the uncracked concrete tension zone, c_{cr}, is determined by dividing the strain of concrete at cracking by the slope of the strain diagram. The volume of the concrete tensile stress diagram over the area of the uncracked tensile zone is then calculated to obtain the total force due to tensile concrete stresses. Once the internal forces are computed, the equilibrium is checked by comparing them with the externally applied axial forces. If the equilibrium is satisfied within a prescribed range of accuracy, the assumption for neutral axis location is verified. Otherwise, the neutral axis location is revised and the same process is repeated until the equilibrium is satisfied. Next, the internal moment is calculated and compared with the moment due to the applied loads. If the difference is smaller then an assumed tolerance value, the analysis is stopped, otherwise, the program continues the analysis with the next selected extreme compression fiber strain. At the end of the analysis the extreme fiber compression strain is divided by the distance to neutral axis to calculate the inelastic curvature, Φ.

Cross-section   Strain diagram   Forces
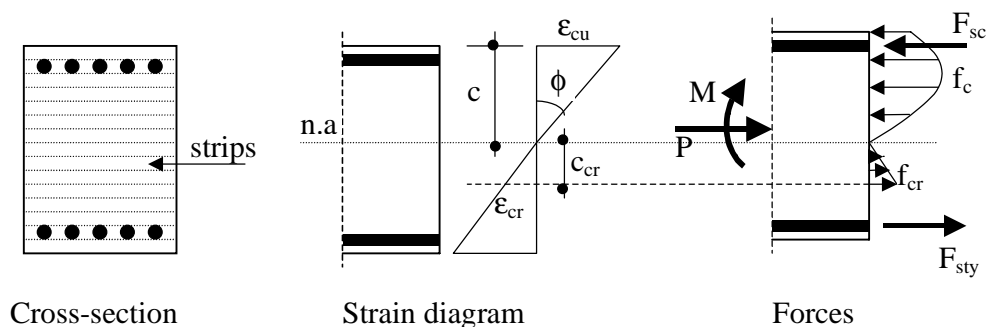
Fig. 8 - Internal strains and stresses at abutment cross-section

5. Implemented LSD analysis procedure

In the program, the following SLS and ULS conditions are considered for geotechnical and structural design of the abutment..

Geotechnical:
- SLS soil resistance for shallow foundations or SLS pile axial resistance for deep foundations,
- ULS soil resistance for shallow foundations or ULS pile axial resistance for deep foundations,
- Structure stability for sliding and overturning at ULS

Structural:
- Crack width limitations for concrete at SLS
- Shear and flexural strength of the abutment at ULS

The ULS conditions are checked using separate factors of safety on loads and structure resistance. The ULS load combinations and maximum and minimum values of load factors are shown respectively in Tables 1 and 2 [22]. Table 3 tabulates the resistance factors for various geotechnical ULS conditions [22] used in the program. The SLS conditions for abutments are checked using unfactored loads and structure resistance. The load combination used in the program for SLS is also illustrated in Table 1.

The three-dimensional effects of applied loads and structure weight, including the weight of the wing-walls, are considered in the program for the geotechnical and structural design of the abutment foundation. For sloping backfill soil conditions, the effect of vertical component of earth pressure is also considered in the foundation's design. The total weight of the backfill soil,

including the sloping part, is averaged as a uniformly distributed load and applied on the footing's top surface. The procedure used in the program for the structural and geotechnical analysis of the structure components is described in the following sub-sections.

Optimization of Load Effects

In the program, each load is input separately with an identification number (ID) and a type ID as shown in Table 2. The load effects are factored and combined according to their type ID using the load combinations in Table 1. Each load may have more than one case of application, or load-case. For example, to define the possible detrimental effects of live load on an abutment footing, more than one load case may be considered to maximize the effects of sliding, overturning and base pressure. Obviously, these cases can not be combined simultaneously as they belong to the same live load applied at various locations on the bridge. Nevertheless, the one, which results in the most detrimental effect, is output as an envelope response.

For the analysis of the abutment, a maximum and a minimum factored horizontal load is combined with a maximum or a minimum factored vertical load. The combinations that result in the most detrimental load effect are used for geotechnical and structural resistance checks. The correlation between the minimum and maximum load factors shown in Table 2 for permanent loads is considered when combining the loads to optimize their detrimental effect on the structure. For example, the maximum load factor for lateral earth pressure loading is used with the minimum load factor for the structure weight to maximize the effect of overturning. However, in another case, the maximum load factor for structure weight is considered when maximizing the effect of axial load on piles for deep foundations. Some transient loads are also removed if their effect is counteracting the detrimental effect of other applied loads. For example, the live load on the structure is removed if its effect is favourable to the strength or stability of the structure. It is noteworthy that all possible load combinations are considered regardless of their resulting effects on the structure. However, at the end, the envelope responses due to such load combinations are used to check if the structure has adequate resistance to endure the applied loads.

Base Pressure Calculations for Shallow Foundations

The forces applied on a foundation produces horizontal and vertical stresses in the ground. The aim of shallow foundation design is to ensure that those stresses do not exceed the ultimate resistance of the foundation soil and do not cause deformations that will affect the serviceability of the structure. Accordingly, for abutments with shallow foundations, two sets of soil pressure limits are used in the program to check the geotechnical capacity of the bearing soil. One of them is expected to satisfy the resistance aspect at ULS and the other one is expected to satisfy the criteria associated with the tolerance of either the soil or the structure to deformation at the SLS [22]. The program analyzes the abutment foundation for both ULS and SLS conditions. The condition, which yields the lower of the values for factored geotechnical resistance at ULS or geotechnical reaction at SLS, then governs the geotechnical design of the foundation.

For the ULS design of abutment footings, a contact pressure of uniform distribution is assumed such that the centroid of the vertical component of the applied load coincides with the vertical component of the bearing pressure as shown in Fig. 9. Accordingly, the dimensions, b_1 and b_2 of the uniform pressure block, are expressed in the program as follows:

$$b_1 = B_1 - 2e_1 \tag{14}$$

$$b_2 = B_2 - 2e_2 \tag{15}$$

Where, B_1 and B_2 are the plan dimensions of the footing and e_1 and e_2 are the eccentricities of the applied load parallel to B_1 and B_2 faces of the footing. It is noteworthy that the effect of

lateral forces acting on the footing surface is carried to the base of the foundation when calculating the eccentricities [31]. The ULS base pressure, q_f , due to a factored eccentric resultant vertical load, P_{Rf}, on the footing, is then calculated as follows:

$$q_f = \frac{P_{Rf}}{b_1 \times b_2} \tag{16}$$

Where, q_f represents a minimum resistance expected from the soil and it is compared with the ultimate bearing resistance, q_u, of the foundation soil. In the program, the effect of horizontal load on the ultimate bearing resistance of the foundation soil is taken into consideration using a reduction factor, R, expressed as follows:

$$\left\{ \begin{array}{lll} Cohesive\ soil & & R = 1 - 1.30x + 0.57x^2 \\ & D \div b = 0.125 & R = 1 - 2.76x + 2.22x^2 \\ & D \div b = 0.25 & R = 1 - 2.50x + 1.80x^2 \\ Non-cohesive\ soil & D \div b = 0.50 & R = 1 - 2.20x + 1.50x^2 \\ & D \div b = 1.00 & R = 1 - 1.92x + 1.22x^2 \\ & D \div b = 2.00 & R = 1 - 1.63x + 0.94x^2 \end{array} \right\} \tag{17}$$

Where, D, is the depth of the soil in front of the abutment measured to the base of the footing, b is the effective width of the ULS pressure block in the direction of interest and x is the ratio of the factored horizontal load to vertical load. The above expression is based on Meyerhof's [32,33] bearing resistance equations for an angle of internal friction of 30°. The user-input ultimate bearing resistance is adjusted by dividing it by the reduction factor calculated using the above expression. In the program, linear interpolation is used to obtain the reduction factors for values of D/b other then those defined in the above equation.
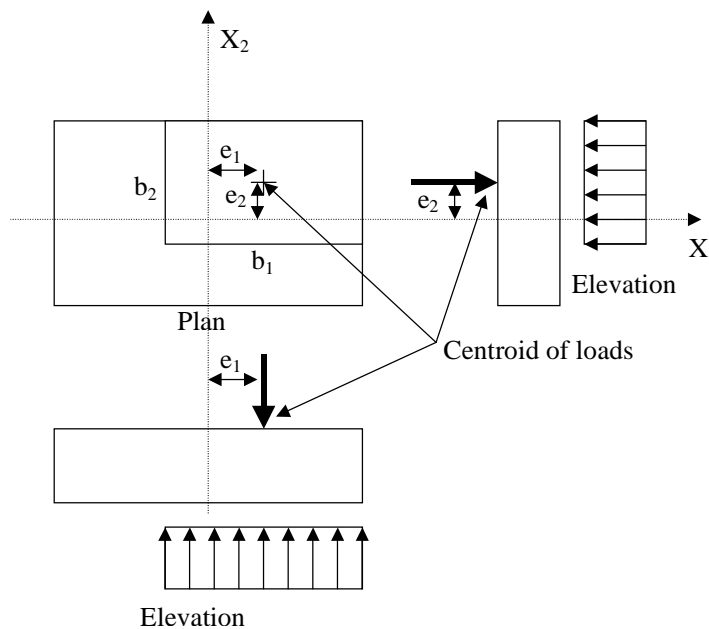

Fig. 9 - Base pressure at ULS

Equation 17 indicates that the ultimate bearing resistance of the foundation soil is a function of the applied loads. Accordingly, in the program, the load combination, which causes the most detrimental effect, is obtained by optimizing the ratio of ultimate base pressure to ultimate bearing resistance.

For the SLS design of abutment footing, the foundation soil is assumed to respond elastically. Consequently, a linear elastic distribution of contact pressure is used in the analysis. The abutment footing is assumed to be infinitely rigid for analysis purposes. In the program, the SLS pressure, q, at the footing corners is first calculated using the following equation and assuming that all corners are in compression.

$$q = \frac{P_{Rf}}{A} \pm \frac{M_{Rf1}}{S_1} \pm \frac{M_{Rf2}}{S_2} \qquad (18)$$

Where A is the plan area of the footing, M_{Rf1} and M_{Rf2} are the resultant moments, respectively about X1 and X2 footing local axes, due to the applied loads and S_1 and S_2 are section modulus of the footing about X1 and X2 footing local axes. If the above expression results in a tensile pressure at one or more corners of the footing, then, the expressions derived by Wilson [34] are used in the analysis. Wilson [34] presented three sets of equations to calculate the actual pressure distribution for the cases where one, two and three corners of the footing are in tension. In the program, for each load combination, the maximum of the calculated SLS base pressure at four corners of the footing is stored in an array. The load combination, which causes the most detrimental effect, is then obtained by optimizing the ratio of the maximum SLS base pressure to user-input SLS bearing resistance.

Resistance of Shallow Foundations to Horizontal Loads

For the ULS design of abutment footings resting on soil, the sliding failure at the interface between the footing and the soil is considered in the program. The resistance of the footing to sliding is generated by the passive earth pressure in front of the abutment as well as cohesion and friction at the footing-soil interface. The contribution of the passive earth pressure in front of the abutment is generally neglected in the calculation of sliding resistance since there is always a possibility that the soil could somehow be disturbed. Accordingly, the following equation is used in the program to calculate the resistance, H_r, of the footing to sliding.

$$H_r = A_e C_{ar} + P_{Rf} \tan\phi \qquad (19)$$

Where, A_e is the effective area of contact pressure, C_{ar} is the factored apparent cohesion and ϕ is the angle of friction. In the program, the load combination, which causes the most detrimental effect, is obtained by optimizing the ratio of factored horizontal load to factored sliding resistance of the foundation.

Stability of Shallow Foundations

In the program, at the ULS, the eccentricity of the vertical load is restricted to 30% of the footing dimension in the direction of the eccentricity [22]. This is done to limit the local bearing stresses in the soil to avoid the possibility of a bearing failure towards the rear of the footing or overturning. The eccentricity of the factored vertical load is first calculated for each load combination. The ratio of this eccentricity to the calculated eccentricity limit is optimized in the program to determine the load combination, which causes the most detrimental effect.

Calculation of Pile Forces for Deep Foundations

For abutment footings resting on piles, assuming that the pile-cap is infinitely rigid, the axial force, N_i, in pile, i, is calculated using the following equation:

$$N_i = \frac{P_{Rf}}{n_p} \pm \frac{M_{Rf1}}{I_{p1}} x_{2i} \pm \frac{M_{Rf2}}{I_{p2}} x_{1i} \qquad (20)$$

Where n_p is the number of piles, x_{1i} and x_{2i} are the distances of pile i from the local footing axes origin respectively in X1 and X2 directions. The moments of inertia of pile group, I_{p1} and I_{p2} respectively about X1 and X2 footing local axes are expressed as:

$$I_{p1} = \sum_{1}^{n_p} x_{1i}^2 \qquad (21)$$

$$I_{p2} = \sum_{1}^{n_p} x_{2i}^2 \qquad (22)$$

The axial force, N_{bi}, on a battered pile i, is then obtained using the following equation:

$$N_{bi} = N_i \sqrt{1 + \frac{1}{b_p^2}} \qquad (23)$$

Where, b_p is the pile batter. In the program, the load combination, which causes the most detrimental effect, is obtained by optimizing the ratio of calculated pile axial load to the geotechnical axial capacity of the pile.

Resistance of Deep Foundations to Horizontal Loads

The horizontal forces acting on the footing are resisted by the pile batters and the reaction forces produced upon horizontal movement of the foundation. The passive earth pressure in front of the piles as well as the shear forces resulting from pile displacement produces this latter resistance. Due to the complex nature of soil-pile interaction, which is a function of various parameters such as number of pile rows, pile spacing etc. [35], this horizontal resistance is not calculated by the program and is provided by the user. However, the horizontal resistance due to the pile batters is calculated in the program as the sum of the horizontal components of calculated axial forces on battered piles. The total horizontal resistance is then obtained in the program by summing up the calculated horizontal resistance due to pile batters and the user-input horizontal resistance of the pile group.

Structural Analysis of Footing

For the structural analysis of the footing, two different ULS soil pressure distributions are considered in the program. The first case considers a contact pressure distribution due to yielding soil, which approximates a uniform pressure distribution over an effective area, as explained previously. This pressure distribution is primarily used to check the bearing resistance of the soil. However, the abutment footing is also structurally designed to sustain such a pressure. The second case assumes a nearly rigid footing and a linear contact pressure distribution due to an elastic non-yielding soil where the probable resistance of soil may exceed the ultimate resistance used in geotechnical design. The program then calculates the flexural and shear forces in the footing for each contact pressure distribution. Larger of the structural responses obtained from both cases will then govern the structural design at ULS. For the SLS condition, only a linear contact pressure distribution is assumed. In the case of deep foundations, flexural and shear forces in the footing are calculated using the previously calculated SLS and ULS pile axial forces.

Normally, the program calculates flexural forces at both faces of the abutment wall and shear forces at a distance 0.9 times the footing thickness from both faces of the abutment wall. Additional sections can be specified by the user around pile locations in the case of deep foundations. The calculated flexural and shear forces are then divided by the width of the footing to obtain the effect of such forces per unit width. The structural resistance calculations are then performed at the same response locations by the program's resistance module.

Structural Analysis of Abutment Wall

In the program, the abutment wall is modeled as a cantilever having a unit width in the transverse direction and a variable thickness in the longitudinal direction of the bridge. The point of fixity of the cantilever model is assumed at the footing's top surface. The loads acting

on the structure are proportioned to the abutment's unit width and applied on the model. In the program, the ballast wall and the breast wall are divided respectively into 5 and 10 prescribed locations spaced equally along the abutment height. The responses due to each applied load are first calculated at these prescribed locations starting from the top and then combined using Table 1. The structural resistance calculations for the abutment are also performed by the program's resistance module at the same prescribed locations considering the combined effects of axial, shear and flexural forces.

Structural Resistance Calculations

The optimum flexural resistance of a reinforced concrete section is a function of the applied axial force and the extreme fiber compression strain [36, 37]. To calculate the flexural resistance of a cross section along the structure for a prescribed axial force, the extreme fiber compression strain, ε_{cu}, for concrete is varied between 0.0020 and 0.0035 using an incremental step of 0.0001. For each incremental strain value, the slope of the strain diagram is established for an assumed location, c, of neutral axis measured from the top of the section as shown in Figure 8. Corresponding compressive and tensile stresses in concrete and steel are determined from material models described previously. Internal forces in concrete, as well as reinforcing steel are calculated. The equilibrium is checked by comparing the resultant internal force with the externally applied axial force. If the equilibrium is satisfied within a prescribed range of accuracy, the assumption for neutral axis location is verified. Otherwise, the neutral axis location is revised and the same process is repeated until the equilibrium is satisfied. Next, the internal moment is calculated and stored in an array. The program then continues the analysis with the next selected extreme compression fiber strain until it reaches the maximum value of 0.0035. At the end of the analyses, the maximum of the stored moments is selected as the flexural resistance of the section.

The compression field theory [22,38] is implemented in the program to calculate shear resistance of a cross section on the structure. The shear resistance, V_r, of a reinforced concrete section without transverse reinforcement is defined as [22]:

$$V_r = \beta \phi_c f_{cr} b_v d_v \tag{24}$$

where, β is a dimensionless parameter, ϕ_c is the resistance factor for concrete, b_v and d_v are respectively the effective section width and depth used in shear resistance calculations. To calculate β, the angle of inclination, θ, of principle compressive strain or shear cracks is varied between 27° and 79° using an incremental step of 1° in the program. For each incremental value of θ, the reinforcement tensile strain, ε_x, is calculated using the following equation:

$$\varepsilon_x = \frac{0.5\left(P_f + V_f Cot\theta\right) + \dfrac{M_f}{d_v}}{E_s A_s} \geq 0 \tag{25}$$

Where, P_f, V_f and M_f are respectively the factored axial load, shear and moment acting on the cross section and E_s and A_s are respectively the modulus of elasticity and area of reinforcing steel. Then, the principal tensile strain, ε_1, and β are calculated as:

$$\varepsilon_1 = \varepsilon_x \left(1 + \cot^2 \theta\right)$$

$$\beta = \frac{0.36}{0.3 + \dfrac{0.69 d\varepsilon_1}{\sin\theta}} \leq \frac{0.66 \cot\theta}{1 + \sqrt{500\varepsilon_1}} \tag{26}$$

Where, d is the distance of tensile reinforcement from the extreme compression fibre. The value of β is stored in an array and the procedure is repeated for the next incremental value of θ until it reaches the maximum value of 79°. At the end of the analysis, the maximum of the stored β values is used in Equation 24 to calculate the shear resistance of the section.

6. Design-aid for cantiliver retaining walls

The program, ABA, is used to obtain the design-aid Tables 4-9 for cantilever retaining walls. The tables are used in conjunction with Figures 10 and 11. The design-aid tables are generated for a granular backfill material with a unit weight of 22 kN/m^3 and an angle of internal friction of 30°. This backfill material is commonly used in transportation structures [22]. The unfactored SLS and ULS bearing resistances of respectively 250 kPa and 750 kPa are used for the foundation soil as conventional design values. The effective angle of friction for the foundation soil is assumed as 30°. The compressive strength of concrete is 30 MPa and the yield strength of steel is 400 MPa. Hydrostatic pressure is not included in the analysis assuming that the water will be properly drained throughout the granular backfill material.

In Fig. 10, q_1 and q_2 are the maximum bearing pressures assuming respectively a linear pressure distribution at SLS and a uniform pressure distribution at ULS. V and P are respectively the total ULS vertical and horizontal forces obtained for the most critical load combination for sliding. In Figure 11, each set of bars is indicated by a letter. The number of T bars are for each face of footing or wall. The maximum spacing of T bars is 300 mm and the lap is 600 mm. The dimensions in the figure are in mm.
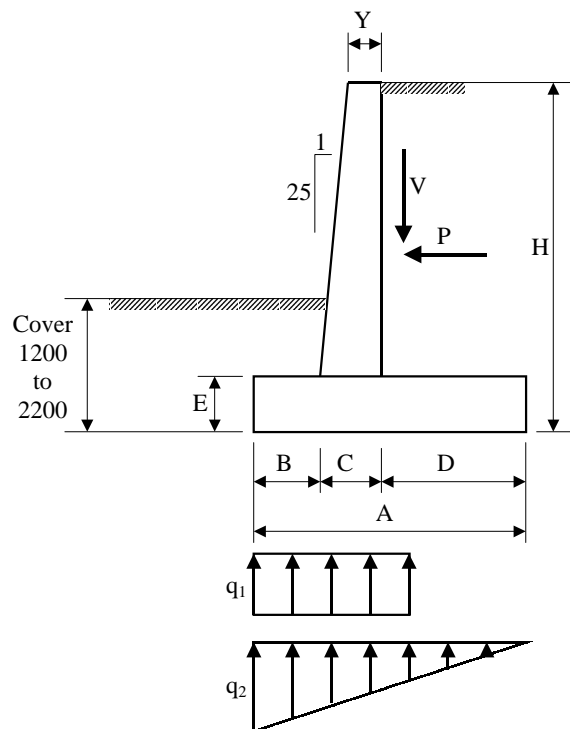
Fig. 10 - Retaining wall dimension parameters

Tables 4 and 5 provide design-aid for cantilever retaining walls with zero surcharge pressure and level backfill slope. Table 4 provides dimensions of the wall as a function of its height for 1200 mm and 2200 mm toe soil cover to frost depth. Table 5 provides the length, size and spacing of reinforcement as well as steel and concrete quantities as a function of wall height. Tables 6 and 7 provide similar design-aid for cantilever retaining walls with a live load surcharge pressure of 13.2 kPa, a commonly used design parameter in North America. Tables 8 and 9 provide design-aid for cantilever retaining walls with a backfill slope of 2 horizontal to 1 vertical.
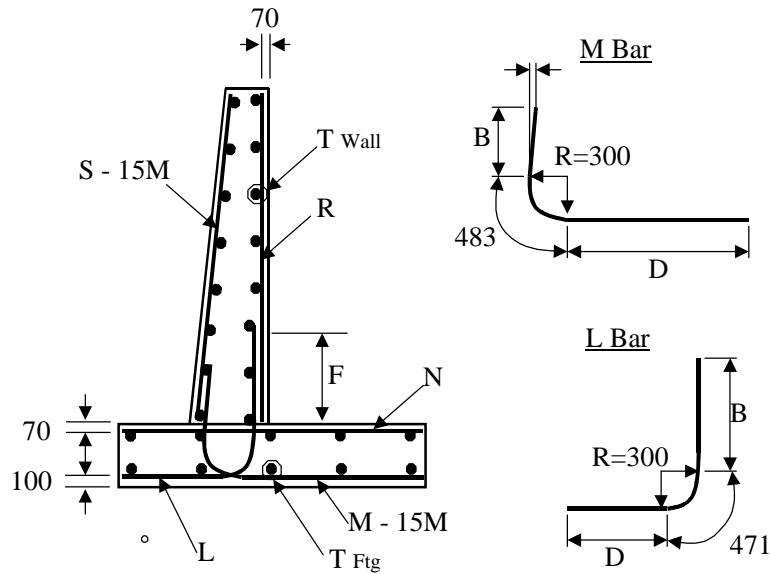
Fig. 11 - Retaining wall reinforcement parameters

7. Conclusions

A computer program, developed for the limit states analysis of bridge abutments, is presented in this paper. Although several other computer programs exist for the analysis of bridge abutments, they are limited to cases where working stress design approach is used for the geotechnical analysis of the structure. Different from these conventional programs, the developed program is able to perform both structural and geotechnical analysis of bridge abutments and check their resistance to calculated responses using limit states design criteria. In the program, the earth pressure coefficient for the backfill soil is calculated as a function of abutment's lateral displacement taking into consideration the non-linear force-deformation relationship of the structure. Therefore, for abutments partially restrained against lateral movement, an earth pressure coefficient less than that of at-rest conditions may be obtained. This may result in a more economical design. Design-aid charts for cantilever retaining walls are also generated using this program.

REFERENCES

1. Meyerhof, G.G. Safety factors in soil mechanics. Canadian Geotechnical Journal 1970; 7: 349-355.
2. Meyerhof, G.G. Limit states design in geotechnical engineering. Structural Safety 1982; 1: 67-71.
3. Meyerhof, G.G. Safety Factors and limit states analysis in geotechnical engineering. Canadian Geotechnical Journal 1984; 21: 1-7
4. Meyerhof, G.G. Development of geotechnical limit state design. Proceedings of the International Symposium on Limit State Design In Geotechnical Engineering . Copenhagen: Danish Geotechnical Society, 1993; 1: 1-12.
5. Meyerhof, G.G. Development of geotechnical limit state design. Canadian Geotechnical Journal 1995; 32: 128-136.
6. Lumb, P. Safety factors and probability distribution of soil strength. Canadian Geotechnical Journal 1970; 7: 225-242.
7. Allen, D. E. Limit States Design - A probabilistic study. Canadian Journal of Civil Engineering 1975; 2: 36-49.
8. Allen, D. E. Limit states criteria for structural evaluation of existing buildings. Canadian Journal of Civil Engineering 1991; 18: 995-1004.

9. MacGregor, J.G. Safety and limit states design for reinforced concrete. Canadian Journal of Civil Engineering 1976; 3: 484-513.

10. Bolton, M. D. Limit state design in geotechnical engineering. Ground Engineering 1981; 14(6): 39-46.

11. Balkie, L. D. Total and partial factors of safety in geotechnical engineering. Canadian Geotechnical Journal 1985; 22: 477-482.

12. Ovesen, N.K. Towards an european code for foundation engineering. Ground Engineering 1981; 14 (7): 25-28.

13. Ovesen, N.K. Eurocode 7: An european code of practice for geotechnical design. Proceedings of the International Symposium on Limit State Design In Geotechnical Engineering. Copenhagen: Danish Geotechnical Society, 1993; 3: 691-710.

14. Ovesen, N. K. and Orr, T. Limit States Design: the european perspective. Proceedings of Geotechnical Engineering Congress 1991. American Society of Civil Engineers, 1991; Special Publication No 27, 2: 1341-1352.

15. Green, R. The development of a LRFD code for Ontario bridge foundations. Proceedings of Geotechnical Engineering Congress 1991. American Society of Civil Engineers, 1991; Special Publication No 27, 2, 1365-1376.

16. Green, R., (1993), 'LSD Code for Bridge Foundations', Proceedings of the International Symposium on Limit State Design in Geotechnical Engineering. Copenhagen: Danish Geotechnical Society, 1993; 2, 459-468.

17. Barker, R. M., Duncan, J. M. K., Rojiani, K. B., Ooi, P. S. K, Kim, S.G. Manuals for the design of bridge foundations. NCHRP Report 343. Washington D.C.: Transportation Research Board; National Research Council, 1991.

18. Becker, D. E. Eighteenth Canadian Geotechnical Colloquium: Limit States Design for foundations. Part I. An overview of the foundation design process., Canadian Geotechnical Journal 1996; 33, 956-983.

19. Ontario Highway Bridge Design Code. Third Edition, Ministry of Transportation, Quality and Standards Division, Downsview, Ontario, Canada, 1991.

20. European Code for Standardization. Eurocode 7: Geotechnical design, general rules. Danish Geotechnical Institute, Copenhagen, Denmark, 1992.

21. Associate Committee on the National Building Code. National building code of Canada. National Research Council, Ottawa, Canada, 1995.

22. Canadian Highway Bridge Design Code - Final Draft. Canadian Standards Association, Toronto, Ontario, Canada, 2000.

23. Clough, G. M., Duncan, J. M. Foundation engineering handbook. Fang, H.Y. editor. New York: Van Nostrand Reinhold, 1991.

24. Dicleli, M. A rational design approach for prestressed-concrete-girder integral bridges. Engineering Structures 2000; 22(3): 230-245.

25. Dicleli, M. A simplified structure model for computer-aided analysis of integral-abutment bridges. ASCE Journal of Bridge Engineering 2000; 5(3): 1-9

26. Demetrios, E. T. Bridge engineering: design, rehabilitation and maintenance of modern highway bridges. New York: McGraw-Hill, 1995.

27. Priestly, M. J. N., Seible, F., Calvi, G. M. Seismic design and retrofit of bridges. New York: John Wiley and Sons, 1996.

28. Ghali, A and Neville, A. M. Structural analysis: a unified classical and matrix approach, 3rd edition. New York: Chapman and Hall, 1989

29. Maron, M. J. Numerical analysis: a practical approach, 2nd edition. New York: Macmillan, 1987.

30. Saatcioglu, M. and Razvi, S. Strength and ductility of confined concrete. ASCE Journal of Structural Engineering 1992; 118(9): 2421-2438.

31. Duan, L., (1996), Bridge-column footings: an improved design procedure. ASCE Practice Periodical on Structural Design and Construction 1996; 1(1): 20-24.

32. Meyerhof, G.G. The ultimate bearing capacity of foundations. Geotechnique 1951; 2: 301-332.

33. Meyerhof, G.G. The bearing capacity of foundations under eccentric and inclined loads. Proc., 3rd International Conference on Soil Mechanics and Foundation Engineering. Zurich: 1953; 1: 440-445.

34. Wilson, K. E. Bearing pressures for rectangular footings with biaxial uplift. ASCE Journal of Bridge Engineering 1997; 2(1): 27-33.

35. Rollins, K., Peterson, K. Weaver T. Full scale pile group lateral load testing in soft clay. NCEER Bulletin 1996; October: 9-11.

36. MacGregor, J.G. Reinforced concrete mechanics and design, 2nd edition. New Jersey: Prentice-Hall, 1992

37. McCormac, J. C. Design of reinforced concrete, 4th edition. New York: John Wiley and Sons, 1999.

38. Collins, M.P., Mitchell, D. Prestressed concrete basics. Ottawa: Canadian Prestressed Concrete Institute, 1987.

Appendix

Table 1 -Load factors and load combinations

Limit State	Permanent Loads			Transitory Loads					Exceptional Loads			
	D	E	P	L	K	W	V	S	EQ	F	A	H
SLS-1	1.00	1.00	1.00	0.90	0.80	0.00	0.00	1.00	0.00	0.00	0.00	0.00
ULS-1	α_D	α_E	α_P	1.70	0.00	0.00	0.00	0.00	0.00	0.00	0.00	0.00
ULS-2	α_D	α_E	α_P	1.60	1.15	0.00	0.00	0.00	0.00	0.00	0.00	0.00
ULS-3	α_D	α_E	α_P	1.40	1.00	0.50	0.50	0.00	0.00	0.00	0.00	0.00
ULS-4	α_D	α_E	α_P	0.00	1.25	1.65	0.00	0.00	0.00	0.00	0.00	0.00
ULS-5	α_D	α_E	α_P	0.00	0.00	0.00	0.00	0.00	1.00	0.00	0.00	0.00
ULS-6	α_D	α_E	α_P	0.00	0.00	0.00	0.00	0.00	0.00	1.30	0.00	0.00
ULS-7	α_D	α_E	α_P	0.00	0.00	0.00	0.00	0.00	0.00	0.00	1.30	0.00
ULS-8	α_D	α_E	α_P	0.00	0.00	0.00	0.00	0.00	0.00	0.00	0.00	1.00

A   : Ice accretion load
D   : Dead load
E   : Loads due to earth, surcharge or hydrostatic pressure
F   : Loads due to stream pressure and ice forces or debris torrents
H   : Collusion load
K   : Strains and deformations due to temperature variation, creep and shrinkage
L   : Live load
P   : Secondary prestress load
EQ   : Earthquake load
S   : Load due to foundation deformation
V   : Wind load on traffic
W   : Wind load on structure

α_D : Load factor for load type D
α_E : Load factor for load type E
α_P : Load factor for load type P

Notes

Bar	Area (mm2)	Diameter (mm)
10M	100	11.3
15M	200	16.0
20M	300	19.5
25M	500	25.2
30M	700	29.9
35M	1000	35.7

The yield strength of steel is 400 MPa.

Table 2 - Load types and load factors

Type ID	Definition	LS Group	Load Factor Max.	Load Factor Min.
D1	Factory produced components excluding wood	All	1.10	0.95
D2	Cast-in-place concrete, wood, non-structural comp.	All	1.20	0.90
D3	Wearing surfaces based on nominal thickness	All	1.50	0.65
D4	Earth fill, negative skin friction on piles	All	1.25	0.80
D5	Water	All	1.10	0.90
E1	Passive earth pressure	All	1.25	0.50
E2	At-rest earth pressure	All	1.25	0.80
E3	Active earth pressure	All	1.25	0.80
E4	Backfill pressure	All	1.25	0.80
E5	Hydrostatic Pressure	All	1.10	0.90
P	Secondary prestress effect	All	1.05	0.95
L	Live load	SLS 1	0.90	0.00
		ULS 1	1.70	0.00
		ULS 2	1.60	0.00
		ULS 3	1.40	0.00
K	Loads due to temp. variation, creep and shrinkage	SLS 1	0.80	0.00
		ULS 2	1.15	0.00
		ULS 3	1.00	0.00
		ULS 4	1.25	0.00
W	Wind load on structure	ULS 3	0.50	0.00
		ULS 4	1.65	0.00
V	Wind load on traffic	ULS 3	0.50	0.00
S	Load due to foundation deformation	SLS 1	1.00	0.00
EQ	Earthquake load	ULS 5	1.00	0.00
F	Loads due to stream pressure and ice forces or debris torrents	ULS 6	1.30	0.00
A	Ice accretion load	ULS 7	1.30	0.00
H	Collusion load	ULS 8	1.00	0.00

Table 3 - Geotechnical resistance factors

Foundation Type	Geotechnical Resistance		Factor
Shallow Foundations	Bearing resistance		0.5
	Passive resistance		0.5
	Sliding resistance		0.8
Deep Foundations	Static analysis,	compression	0.4
		tension	0.3
	Static test	compression	0.6
		tension	0.4
	Dynamic analysis	compression	0.4
	Dynamic test	compression	0.5
	Horizontal passive resistance		0.5

Table 4 - **Geotechnical design aid for cantilever retaining walls (surcharge=0, backfill slope=0)**

| | STRUCTURE DIMENSIONS (mm) | | | | | | | GEOTECHNICAL PARAMETERS | | | | | | | | |
| | | | | | | | | Cover = 1200 mm | | | | | Cover = 2200 mm | | | |
H	A	B	C	D	E	Y	P (kN)	V (kN)	$q_{1, SLS}$ (kPa)	$q_{2, ULS}$ (kPa)	R Cohe	R Gran	V (kN)	$q_{1, SLS}$ (kPa)	$q_{2, ULS}$ (kPa)	R Cohe	R Gran
2000	970	300	370	300	300	300	17.3	37.8	86	81	0.53	0.46	---	---	---	---	---
2500	1220	300	390	530	300	300	27.0	58.6	103	97	0.53	0.44	---	---	---	---	---
3000	1470	300	410	760	300	300	38.8	84.7	122	115	0.53	0.42	91.3	139	129	0.55	0.49
3500	1860	540	430	890	350	300	52.8	115.0	114	102	0.53	0.38	126.9	134	119	0.56	0.47
4000	2160	640	540	980	400	400	69.0	150.2	123	111	0.53	0.37	164.3	144	127	0.56	0.46
4500	2460	730	560	1170	450	400	87.3	189.5	133	119	0.53	0.35	205.6	153	135	0.55	0.44
5000	2750	800	580	1370	500	400	107.8	233.9	145	130	0.53	0.34	251.5	165	145	0.55	0.43
5500	3100	940	600	1560	550	400	130.5	283.6	148	134	0.53	0.32	304.3	169	149	0.55	0.41
6000	3360	980	620	1760	600	400	155.3	336.5	163	147	0.53	0.31	358.1	183	162	0.55	0.40
6500	3620	1020	630	1970	650	400	182.2	394.7	179	162	0.53	0.30	417.1	199	176	0.54	0.39
7000	3940	1130	650	2160	750	400	211.3	457.9	186	169	0.53	0.29	482.7	206	183	0.54	0.38

Table 5 - Structural design aid for cantilever retaining walls (surcharge=0, backfill slope=0)

H (mm)	L Size	L Spcg	L D	L B	L Spcg	K	M B	M D	N Size	N Spcg	N Lgth	R Size	R Spcg	R Lgth	S Spcg	S Lgth	F Hgt	T (15M) Ftg	T (15M) Wall	Quantity Conc (m³)	Quantity Steel (kg)
2000	15M	300	222	492	300	16	412	222	15M	300	830	15M	300	1550	300	1631	600	4	6	0.86	65
2500	15M	300	242	592	300	16	412	472	15M	300	1080	15M	300	1950	300	2132	700	5	8	1.13	82
3000	15M	300	262	792	300	16	412	722	15M	300	1330	15M	300	2250	300	2632	900	6	10	1.40	99
3500	15M	300	522	1042	300	18	462	872	15M	300	1720	15M	300	2500	300	3082	1100	7	11	1.80	115
4000	15M	250	732	1192	250	20	512	1072	15M	250	2020	15M	250	2850	250	3533	1200	8	13	2.56	147
4500	20M	300	840	1440	300	22	562	1282	20M	300	2320	15M	300	3100	300	3983	1400	9	14	3.05	162
5000	20M	250	930	1590	250	24	612	1502	20M	250	2610	15M	250	3450	250	4434	1500	10	16	3.58	201
5500	20M	250	1090	1840	250	26	662	1712	20M	200	2960	15M	250	3700	250	4884	1700	11	17	4.18	227
6000	20M	200	1147	1987	250	28	712	1932	25M	250	3220	15M	200	4050	250	5334	1800	12	19	4.77	284
6500	25M	200	1197	2237	300	30	762	2152	30M	300	3480	15M	200	4300	300	5785	2000	13	20	5.37	327
7000	30M	300	1325	2435	300	34	862	2362	30M	300	3800	20M	300	4720	300	6185	2100	14	22	6.24	350

Table 6 Geotechnical design aid for cantilever retaining walls (surcharge=13.2 kPa)

	DIMENSIONS (mm)							GEOTECHNICAL PARAMETERS									
									Cover = 1200 mm					Cover = 2200 mm			
H	A	B	C	D	E	Y	P (kN)	V (kN)	$q_{1, SLS}$ (kPa)	$q_{2, ULS}$ (kPa)	R Cohe	R Gran	V (kN)	$q_{1, SLS}$ (kPa)	$q_{2, ULS}$ (kPa)	R Cohe	R Gran
2000	1290	300	370	620	300	300	27.6	60.3	90	80	0.53	0.42	---	---	---	---	---
2500	1530	300	390	840	300	300	39.9	86.9	111	101	0.53	0.41	---	---	---	---	---
3000	1890	500	410	980	300	300	54.3	117.7	111	99	0.53	0.38	128.7	130	114	0.56	0.47
3500	2170	560	430	1180	350	300	70.9	153.6	125	112	0.53	0.36	166.0	143	126	0.55	0.45
4000	2430	590	540	1300	400	400	89.7	194.4	142	128	0.53	0.35	207.4	160	142	0.55	0.44
4500	2730	680	560	1490	450	400	110.6	239.8	153	137	0.53	0.34	254.7	171	151	0.55	0.42
5000	3030	770	580	1680	500	400	133.7	289.6	163	146	0.53	0.32	306.6	181	160	0.54	0.41
5500	3400	940	600	1860	550	400	158.9	344.8	164	148	0.53	0.31	365.5	183	162	0.55	0.40
6000	3750	1090	620	2040	600	400	186.3	403.8	167	152	0.53	0.29	427.7	187	166	0.55	0.38
6500	4040	1170	630	2240	650	400	215.8	467.3	179	163	0.52	0.28	493.1	199	177	0.54	0.37
7000	4320	1230	650	2440	800	400	247.5	536.9	193	175	0.53	0.28	212	212	189	0.54	0.36

Table 7 Structural design aid for cantilever retaining walls (surcharge=13.2 kPa)

	L					M			N			R			S	F	T (15M)		Quantity	
H (mm)	Size	Spcg	D	B	Spcg	K	B	D	Size	Spcg	Lgth	Size	Spcg	Lgth	Spcg	Lgth	Hgt	Ftg	Wall	Conc (m³)	Steel (kg)
2000	15M	300	222	492	300	16	412	542	15M	300	1150	15M	300	1550	300	1631	600	5	6	0.95	70
2500	15M	300	242	592	300	16	412	782	15M	300	1390	15M	300	1950	300	2132	700	6	8	1.22	88
3000	15M	300	462	792	250	16	412	942	20M	300	1750	15M	300	2250	250	2632	900	7	10	1.53	120
3500	15M	200	542	1042	300	18	462	1162	20M	250	2030	15M	200	2500	300	3082	1100	8	11	1.91	141
4000	20M	300	680	1190	300	20	512	1392	20M	200	2290	15M	300	2850	300	3533	1200	9	13	2.66	160
4500	20M	250	790	1440	250	22	562	1602	25M	300	2590	15M	250	3100	250	3983	1400	10	14	3.17	195
5000	20M	200	900	1590	300	24	612	1812	25M	250	2890	15M	200	3450	300	4434	1500	11	16	3.72	230
5500	25M	250	1087	1837	250	26	662	2012	25M	250	3260	15M	250	3700	250	4884	1700	12	17	4.35	269
6000	30M	300	1255	1985	300	28	712	2212	30M	300	3610	20M	300	4170	300	5334	1800	13	19	5.00	313
6500	30M	250	1345	2235	250	30	762	2422	30M	250	3900	20M	250	4420	250	5785	2000	14	20	5.64	382
7000	30M	200	1422	2482	250	36	912	2642	30M	250	4180	20M	200	4670	250	6135	2100	15	21	6.71	450

Table 8 - Geotechnical design aid for cantilever retaining walls (backfill slope=2:1)

	DIMENSIONS (mm)							GEOTECHNICAL PARAMETERS											
								Cover = 1200 mm						Cover = 2200 mm					
H	A	B	C	D	E	Y	P (kN)	V (kN)	$q_{1, SLS}$ (kPa)	$q_{2, ULS}$ (kPa)		R		V (kN)	$q_{1, SLS}$ (kPa)	$q_{2, ULS}$ (kPa)		R	
										#1	#2	Cohe	Gran			#1	#2	Cohe	Gran
2000	1460	400	370	690	300	300	36.3	78.7	71	65	72	0.58[#2]	0.38[#1]	---	---	---	---	---	---
2500	2020	630	390	1000	300	300	59.4	128.8	71	71	80	0.58[#2]	0.33[#1]	---	---	---	---	---	---
3000	2590	820	410	1360	300	300	89.4	193.5	74	79	89	0.58[#2]	0.30[#1]	211.6	95	92	105	0.61[#2]	0.40[#1]
3500	3100	850	430	1820	350	300	128.4	278.1	88	94	107	0.58[#2]	0.28[#1]	296.8	107	106	120	0.60[#2]	0.38[#1]
4000	3530	900	540	2090	400	400	168.0	363.9	101	109	123	0.58[#2]	0.27[#1]	383.7	119	119	135	0.60[#2]	0.36[#1]
4500	4010	930	560	2520	450	400	219.0	474.3	117	125	142	0.58[#2]	0.25[#1]	494.7	134	135	153	0.60[#2]	0.34[#1]
5000	4520	1020	580	2920	500	400	275.4	596.6	129	139	157	0.58[#2]	0.24[#1]	619.0	145	148	168	0.60[#2]	0.32[#1]
5500	5040	1130	600	3310	550	400	337.9	731.7	139	151	172	0.58[#2]	0.23[#1]	756.6	155	161	183	0.59[#2]	0.31[#1]
6000	5560	1260	610	3690	700	400	406.2	879.7	148	164	187	0.58[#2]	0.22[#1]	907.5	164	173	197	0.59[#2]	0.30[#1]
6500	6080	1390	630	4060	850	400	480.2	1040.0	157	176	202	0.58[#2]	0.21[#1]	1070.6	173	185	211	0.59[#2]	0.28[#1]
7000	6860	1910	630	4320	1150	400	553.8	1199.2	138	171	207	0.58[#2]	0.20[#1]	1241.0	157	182	214	0.59[#2]	0.27[#1]

Table 9 - Structural design aid for cantilever retaining walls (backfill slope=2:1)

H (mm)	L								N			R			S		F	T (No.)		Quantity	
	Size	Spcg	D	B	Spcg	K	B	D	Size	Spcg	Lgth	Size	Spcg	Lgth	Spcg	Lgth	Hgt	Ftg	Wall	Conc (m³)	Steel (kg)
2000	15M	300	322	492	300	16	412	612	15M	300	1320	15M	300	1550	300	1631	600	6	6	1.01	76
2500	15M	300	572	592	300	16	412	942	15M	250	1880	15M	300	1950	300	2132	700	8	8	1.37	107
3000	15M	250	782	792	250	16	412	1322	20M	250	2450	15M	250	2250	250	2632	900	10	10	1.74	158
3500	20M	300	830	1040	300	18	462	1802	25M	300	2960	15M	300	2500	300	3082	1100	11	11	2.23	196
4000	20M	300	990	1190	300	20	512	2182	25M	300	3390	15M	300	2850	300	3533	1200	13	13	3.10	241
4500	20M	250	1040	1440	250	22	562	2632	25M	250	3870	15M	250	3100	250	3983	1400	14	14	3.75	304
5000	20M	200	1147	1587	300	24	612	3052	25M	250	4380	15M	200	3450	300	4434	1500	16	16	4.47	407
5500	25M	250	1277	1837	250	26	662	3462	30M	300	4900	20M	250	3820	250	4884	1700	18	17	5.25	492
6000	30M	300	1415	2085	300	32	812	3852	30M	300	5420	20M	300	4070	300	5234	1800	19	19	6.57	530
6500	30M	250	1565	2335	250	38	462	4242	30M	300	5940	20M	250	4320	250	5584	2000	21	20	8.08	615
7000	30M	250	2085	2735	250	50	1263	4502	25M	250	6720	20M	250	4420	250	5785	2000	24	20	10.90	635